

rapid circulation of liquid around the bubbles. The general flow pattern is shown in Fig. 1 (left).

The liquid moved along the heated surface toward the bubble from all sides, and then traveled downward around the bubble periphery and was exuded downward in a stream from the bottom extremity of the bubble.

In larger apparatus the stream of liquid leaving the bubble surface has been observed to reach a length of 5 cm. The bubbles in this case were formed in highly subcooled liquid and were observed by 8000-frame-per-second photography to have a constant volume and to be non-oscillating over a time period of a minute or more.

As new bubbles grew at the preferred nucleation sites, they very quickly established the same characteristic liquid flow pattern. The velocity of the liquid around the bubble was of the order of 1 to 2 cm/sec when vigorous boiling was occurring. At lower boiling rates the liquid was not pushed away from the bubble so vigorously; rather, there was a tendency to produce rotating vortices near the heating surface. The bubbles were not observed to move downward from the heating surface, nor were they observed to oscillate, but on the contrary they maintained a stable shape for a number of seconds. Some of the bubbles could be observed moving along the heating surface, and a tendency for the bubbles to move toward each other was apparent.

Observations of a large number of stable, nongrowing air bubbles under nonboiling conditions show that the characteristic liquid flow patterns are essentially identical to those observed for vapor bubbles obtained under boiling conditions. Figures 1 and 2 show typical liquid flow patterns around stable air bubbles that were placed on the heating surface. The photographs are time exposures, so the illuminated particles appear as streaks indicating flow streamlines. These air bubbles reached their stable shape essentially immediately after the temperature gradient was established, and maintained this shape for periods often exceeding 2 minutes.

An additional observation showed that when two air bubbles were placed on the plate in the vicinity of one another they tended to coalesce in a manner similar to that observed for vapor bubbles. The reason for the coalescent tendency became obvious when we ob-

served the liquid flow patterns around the bubbles.

The liquid between the bubbles becomes quickly heated because of the increased thermal mixing in that region, thus a horizontal temperature gradient is established. The horizontal temperature gradient and attendant horizontal surface tension gradient result in liquid flowing generally from the hotter toward the colder region, with a resultant bubble motion in the opposite direction.

The net result of the Marangoni flow around bubble surfaces significantly contributes to the convection of liquid away from the heated surface. Thus the Marangoni flow serves as a primary factor in the heat transfer mechanism for those situations in which bubbles remain on the heating surface for a relatively long period of time. As such, it may replace or supplement the currently recognized mechanism of liquid agitation resulting from bubble formation and separation from the heating surface.

Brightness Distributions of Radio Sources at 2-Centimeter Wavelength

Abstract. Maps have been made of the 2-centimeter brightness distribution of M17, Cassiopeia-A, Taurus-A, and Orion nebula with a resolution of 2.3 minutes of arc, revealing several newly resolved features. M17 is a double thermal source. Some structure appears in Cassiopeia-A, including a suggestion of a ring shape. Taurus-A exhibits a brightness map similar to that obtained in earlier low-frequency results. The central part of Orion nebula is circularly symmetric to a high degree of accuracy.

The newer instruments for the study of the continuum radiation from discrete radio sources are designed to increase the resolution and to extend the observable radio-frequency spectrum. Data obtained with these instruments can be used to test current theories of the origins and radiating mechanisms of H_{II} regions and supernova remnants within the galaxy, and to find out more concerning extragalactic emitters of radio waves. We report the observations on mapping of four bright sources at a wavelength of 2 cm, using the 2.3-minute-of-arc beam of the 36-m parabolic reflector at the Haystack Research Facility.

The tuned radio frequency receiver amplified and detected signals in a passband from 2.0 to 1.875 cm (15 to 16 Ghertz). The equivalent

From the identical flow patterns observed around the surfaces of air bubbles and boiling-produced vapor bubbles, it can be concluded that Marangoni liquid flow will occur around any bubble located in a temperature gradient.

JAY L. MCGREW

FRANK L. BAMFORD

*Martin Company,
Denver, Colorado*

THOMAS R. REHM

*University of Denver,
Denver, Colorado*

References and Notes

1. C. S. M. Marangoni, *Nuovo Cimento Ser.* 2, 516, p. 239 (1872).
2. L. E. Scriben and C. V. Sternling, *J. Fluid Mech.* 19, 321 (1964).
3. W. M. Rohsenow and H. Y. Choi, *Heat, Mass and Momentum Transfer* (Prentice-Hall, Englewood Cliffs, N.J., 1961), p. 211; L. S. Tong, *Boiling Heat Transfer and Two-Phase Flow* (Wiley, New York, 1965), p. 5.
4. F. D. Moore and R. B. Mesler, *A.I.Ch.E. (Am. Inst. Chem. Engrs.) J.* 7, 620 (1961).
5. F. Gunther and F. Kreith, "Photographic study of bubble formation in heat transfer to subcooled water," Progress Report 4-120, Jet Propulsion Laboratory, California Institute of Technology, 1950.
6. Supported by NASA contract NAS8-11328.

14 April 1966

temperature of the noise power generated by the receiver was about 1500°K, which resulted in a fluctuation of the output that was equivalent to 0.04°K rms for the 8-second integration time used. The two-dimensional smoothing process reduced the fluctuation from the receiver output to much less than 0.01°K. This uncertainty was negligible compared with the systematic errors in aligning the scans and determining the baseline temperatures due to sky background, which are estimated to be $\pm 5^\circ\text{K}$ peak and are clearly seen as a regular undulation in the lowest contours on several of the maps.

The antenna was on an altazimuth mounting and was pointed to follow and to scan celestial objects by means of a digital computer. The computer

was programmed to scan the beam of the telescope over a rectangular raster of sky centered on the assumed position of the radio source. The line scans extended far enough beyond the source to provide measurements of baseline temperatures. A smooth baseline was obtained by interpolating the array of baseline points; the background temperature was considered a function of elevation only. The maps were assembled from the original line scans, and smoothed by a Fourier transform process that removed all spatial frequencies higher than those that the beam of the telescope could have passed. The brightness temperatures were finally corrected for the measured efficiency of the radio telescope (0.23). In the cases of M17 and Orion, the indicated brightness values are equal to the brightness temperatures of the presumably unpolarized radiation. Because Taurus-A was known to be polarized and since there was also some possibility of detecting polarization in Cassiopeia-A at this short wavelength, these sources were mapped at an hour angle of approximately 6 hours, with the E -vector of the antenna feed within $\pm 5^\circ$ of position angle 90° , throughout the observations. The maps

represent the radio brightness of that component of the total radiation from the sources, averaged over the 1000-Mhertz passband of the receiver.

The outstanding feature of the map of M17 (Omega nebula, Fig. 1) is clearly the second source, about 3.5 minutes of arc from the main source in position angle 20° . The existence of a second source was suggested by earlier fanbeam observations with high resolution only in the east-west direction (1, 2). Apparently the small position angle of the line joining the components, coupled with the east-west elongation of the northern component, made it difficult to produce a clear picture of M17 with such instruments, in spite of the relatively small difference in the fluxes (about 3 to 5).

It is evident from Fig. 1 that we cannot make a simple calculation of the electron density by assuming a simple spherical or cylindrical symmetry for the gas distribution. The resulting values would be too low at the center of either component. However, we have computed the emission measures $E(O)$ through the center of each of the components, following the analysis of Menon (3) and assuming an electron temperature of 10^4 K and an opti-

cal thickness much less than 1. We obtain results of 1.4×10^6 and 2.0×10^6 for the peaks of the weaker and stronger components respectively, or about five times larger than those determined by Hobbs (4) and Westerhout (5), who calculated an average value of E over a 5- to 7-minute-of-arc disc.

Cassiopeia-A (Fig. 2) is thought to be a remnant of a supernova explosion that occurred about 1702. The 2.3-minute-of-arc beam was not able to resolve clearly the ring-shaped structure of the source (2, 6), although there is a suggestion of a depression in the center of the map. There is also a small bright region on the edge in position angle 320° and a less well-defined brightening on the opposite edge in position angle 110° , but there is no indication of the depression in the southern part of the brightness distribution that was reported by Baars and Mezger (7).

Possibly the bright spot shows some evidence of the polarization that has been expected, and sought for in vain because of the assumed synchrotron radiation of Cassiopeia-A. We made a series of line scans through the center of the source along position angle 320° by observing over a range of

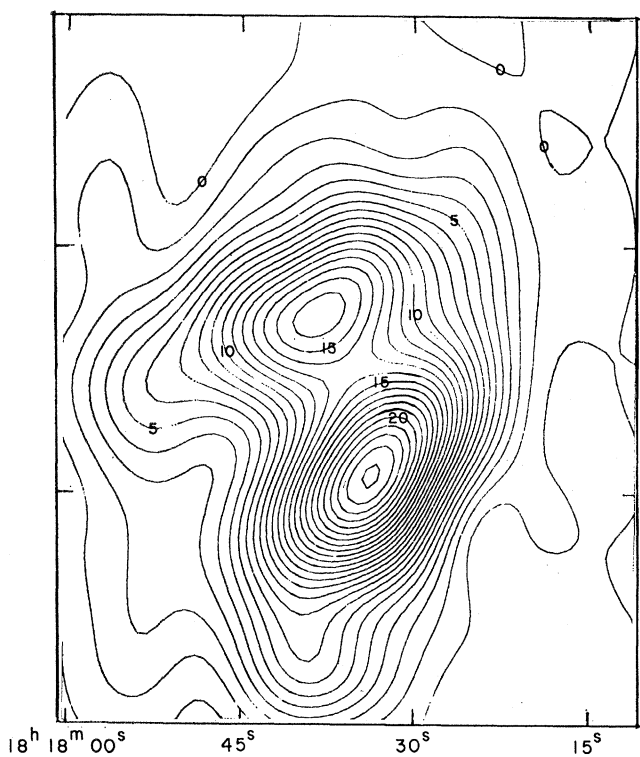


Fig. 1 (above). Omega nebula, 2-cm wavelength; contour interval, 1°K . (1950.0 coordinates.)

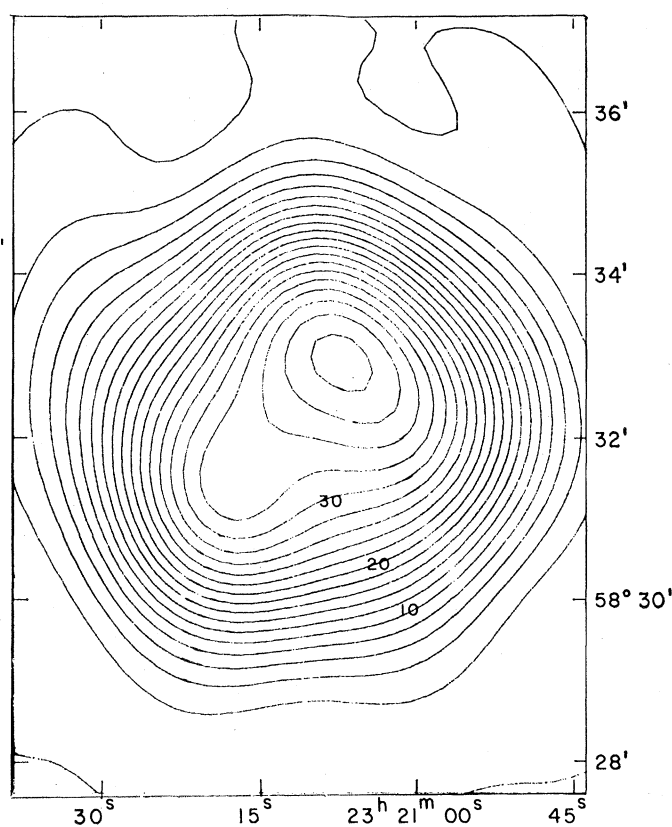


Fig. 2 (right). Cassiopeia-A, 2-cm wavelength; contour interval, 2°K .

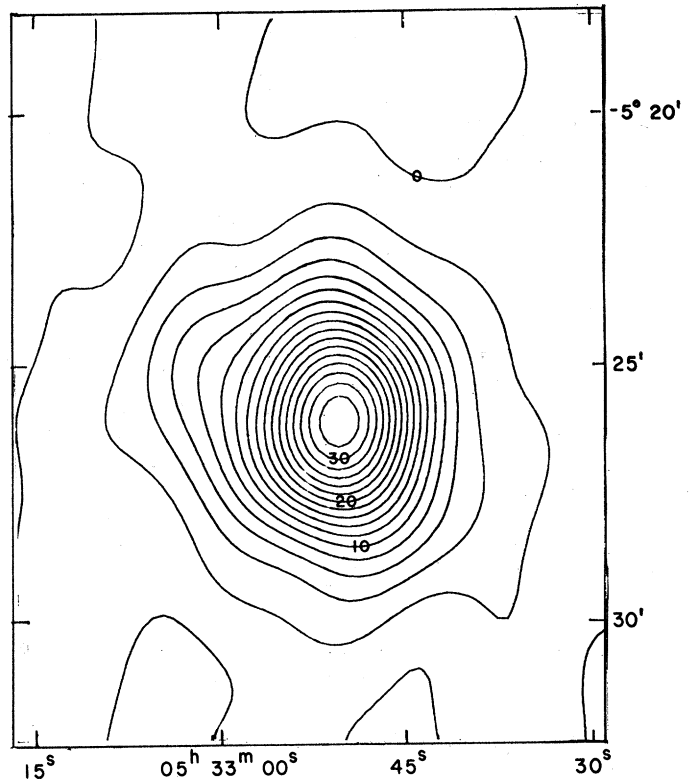
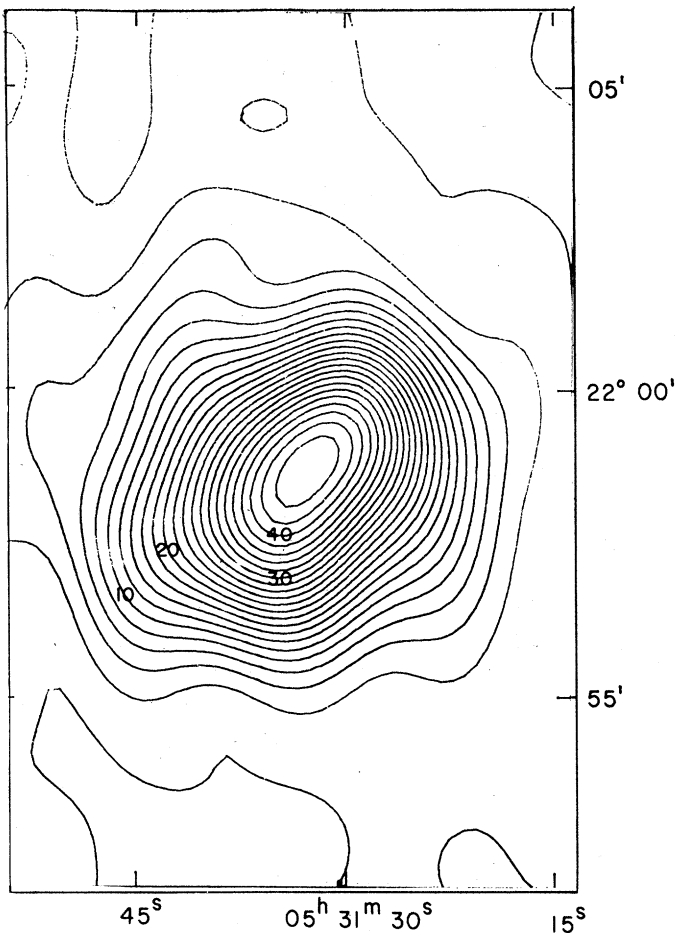


Fig. 3 (left). Taurus-A, 2-cm wavelength; contour interval, 2°K .

Fig. 4 (above). Orion nebula, 2-cm wavelength; contour interval, 2°K .

hour angles. We varied the polarization angle -90° to $+90^\circ$, but in the shape of the scans there was no change that depended on the polarization angle or that exceeded 4°K (out of 39°K —the temperature of the bright peak). Considering that the receiver passband was 1000 Mc wide, a modest amount of Faraday rotation could have caused our negative results.

The 2-cm map of Taurus-A (Fig. 3), another supernova remnant, has the same elliptical contours that have been found at longer wavelengths, that is, a major axis in position angle 135° and half-widths (assuming a Gaussian source and beam shape) of 4.0 and 2.5 minutes of arc. No additional features have appeared at this wavelength and resolution. At the time these measurements were made, there was no simple way to alter the polarization of the telescope, and therefore no attempt was made to compare the complete map of brightness distribution of Fig. 3 with other position angles of polarization.

The emission nebula of Orion (Fig. 4) has an apparent diameter of 3.4 minutes of arc and was therefore well re-

solved by our beam. Nevertheless the brightness distribution appears to be circularly symmetric to a high degree of precision. This finding is strong statistical evidence for the spherical symmetry of the central part of the nebula. If we calculate the average emission measure over the central 1 minute of arc of the source (assuming an electron temperature of 10^4K), we arrive at 3×10^6 , which is the same value as that obtained in the infrared by Moroz (10), and is also in good agreement with Pariiskii (11) and Menon (3), who measured 4×10^6 at 8.3 cm and 2×10^6 at 3.75 cm, respectively. If these values for the emission measure are accepted, there is no need for a small bright central peak as hypothesized by Menon to explain the higher values obtained at optical wavelengths by Strömgren (8). Although such a peak may have contributed to the small discrepancy between my results obtained with a telescope with a resolving power of 2.3 minutes of arc and those at 3.75 cm obtained with a telescope with a resolving power of 6 minutes of arc. Pariiskii's failure to observe

central brightening with the narrow beam of the Pulkovo instrument is enough evidence to deny the existence of this feature.

STANLEY H. ZISK

Research Laboratory of Electronics,
Massachusetts Institute of Technology,
Cambridge, Massachusetts

References and Notes

1. A. G. Little, *Astrophys. J.* **137**, 164 (1963).
2. A. R. Thompson and T. Krishnan, *ibid.* **141**, 19 (1965).
3. T. K. Menon, *Publ. Natl. Radio Astron. Observatory* **1**, 1 (1961).
4. R. W. Hobbs, *Astron. J.* **66**, 517 (1961).
5. G. Westerhout, *Bull. Astron. Inst. Neth.* **488**, 230 *et seq.* (1958).
6. J. Lequeux, *Ann. Astrophys.* **25**, 221 (1962); M. Ryle, B. Elsmore, A. C. Neville, *Nature* **205**, 1259 (1965).
7. J. W. M. Baars and P. Mezger, *Sky and Telescope* **31**, 7 (1966).
8. Strömgren, in *Problems of Cosmical Aerodynamics*, J. M. Burgers and H. C. van de Hulst, Eds. (Central Air Documents Office, Dayton, Ohio, 1951).
9. V. I. Moroz, *Astron. Zh.* **40**, 788 (1963) [Engl. transl.: *Soviet Astron.-AJ* **7**, 601 (1964)].
10. Yu. N. Pariiskii, *Astron. Zh.* **38**, 798 (1961) [Engl. transl.: *Soviet Astron.-AJ* **5**, 611 (1962)].
11. We thank M. L. Meeks of the Haystack Research Facility for use of the telescope, J. C. Henry of the Millstone Hill Radar Facility for use of the computer, and A. H. Barrett and P. G. Mezger for comments and corrections. Supported principally by NASA grant NsG-419.

5 June 1966